

# Magneto-optical investigation of the electronic and magnetic structure of $\text{UAs}_x\text{Se}_{1-x}$

W. Reim, J. Schoenes, and O. Vogt

*Laboratorium für Festkörperphysik, Eidgenössische Technische Hochschule Zürich, CH-8093 Zürich, Switzerland*

(Received 4 October 1983)

The magneto-optical Kerr rotation and ellipticity of different  $\text{UAs}_x\text{Se}_{1-x}$  single crystals has been measured in magnetic fields up to 10 T at variable temperatures for photon energies between 0.5 and 5.7 eV. In addition the optical reflectivity between 0.03 and 12 eV has been determined. The complex diagonal and off-diagonal conductivity tensor elements have been calculated and an interpretation in terms of the electronic structure is presented. We obtain evidence for delocalized narrow  $f$  states with equal bandwidth and similar oscillator strength of the  $f \rightarrow d$  transition in the chalcogenide and the pnictide. A negative conduction-electron spin polarization is found for ferromagnetic USe as well as for UAs in the ferrimagnetic phase. For As-rich compositions, which exhibit a low conduction-electron concentration, we find for the first time in an actinide compound a magnetic red-shift of the  $f \rightarrow d$  transition energy of the order of 150 meV. The total  $f$  moment is shown to consist of antiparallel spin and orbital contributions with a dominating orbital part. Furthermore, we present the determination of the magnetic phase diagram of UAs using the magneto-optical Kerr effect.

## I. INTRODUCTION

UAs and USe form a continuous series of solid solutions crystallizing in the NaCl structure with a nearly constant lattice parameter  $a \approx 5.75 \text{ \AA}$ .<sup>1</sup> UAs is an antiferromagnet with a Néel temperature of  $(125 \pm 2) \text{ K}$ . At about  $\frac{1}{2}T_N$ , it undergoes a first-order phase transition from a  $+-+-$  (type-I) to a  $++--$  (type-IA) stacking of ferromagnetic (001) planes. At this phase transition a 10% decrease of the magnetic moment of the uranium ion has been observed.<sup>2</sup> Recent neutron experiments have shown that the type-IA-to-type-I transition is accompanied by a transition from a  $2\vec{k}$  (easy axis [110]) to a  $1\vec{k}$  (easy axis [100]) collinear spin structure, explaining the change in the magnetic moment.<sup>3</sup> The application of magnetic fields induces intermediate spin structures such as multiple- $\vec{k}$  ferrimagnetic phases.<sup>4</sup>

USe orders ferromagnetically below  $T_C = 160 \text{ K}$ .<sup>5</sup> The easy direction is the (111) axis. No rotation of the magnetization out of this direction could be observed by the application of fields of up to 15 T. This evidences the existence of very strong anisotropy fields.

The complex magnetic behavior of  $\text{UAs}_x\text{Se}_{1-x}$  goes along with an unusual electronic structure. One characteristic feature is the spatially extended nature of the uranium  $f$ -wave functions and their proximity to the Fermi level.<sup>6,7</sup> The metallic conductivity, however, is predominantly due to occupied  $d$  states. A cluster calculation for US has indicated the formation of a dip in the  $d$  density of states near  $E_F$  (Ref. 8) due to the strong  $f$ - $d$  hybridization. In addition, a large  $f$ - $p$  hybridization is expected for the pnictide ( $x = 1$ ), decreasing with decreasing  $x$  because of a shift of the  $p$ -band center to higher binding energies with decreasing covalency.<sup>6,9</sup>

Magneto-optics combined with "normal" optical spectroscopy is well suited for the investigation of the electronic structure a few electron-volts around  $E_F$  due to the

variable and soft excitation energy in the order of the binding energy, and the enhancement of transitions involving "magnetic" electrons in  $\sigma_{xy}$  compared to  $\sigma_{xx}$ . In addition, due to the proportionality of the Kerr signal to sample magnetization, this technique allows a determination of magnetic phase diagrams.

In this paper we present and discuss for the first time magneto-optical results for an uranium pnictide and stress similarities and differences in the electronic structure of uranium chalcogenides and pnictides. Furthermore we present the magneto-optical determination of the magnetic phase diagram of UAs, and discuss the modification of the magnetic structures due to lattice distortion or pressure.

## II. EXPERIMENTAL DETAILS

We have measured the complex polar Kerr effect (rotation  $\theta_K$  and ellipticity  $\epsilon_K$ ) and the optical reflectivity  $R$  for three different  $\text{UAs}_x\text{Se}_{1-x}$  single crystals ( $x = 1, 0.7$ , and 0).<sup>10</sup> The room-temperature reflectivity over a large energy range (0.03–12 eV) was determined under high-vacuum conditions on *in situ* cleaved crystals. Details are described elsewhere.<sup>6</sup> The magneto-optical Kerr measurements have been performed in the (0.5–5.7)-eV energy range on cleaved crystals at variable temperatures (2–300 K). Magnetic fields of up to 10 T were generated by a split-coil superconducting magnet. The field direction is perpendicular to the sample surface in the polar Kerr geometry. The change of light polarization at the near-normal incidence reflection (angle of incidence of less than  $3^\circ$ ) was measured by a zero-compensation lock-in technique using a Faraday modulator for  $\theta_K$  and, in addition, a Soleil-Babinet compensator for  $\epsilon_K$ . The Faraday rotation due to cryostat windows and stray fields has been subtracted by a point-by-point measurement of the sample relative to a reference mirror with a negligible Kerr effect.

The accuracy of this method is better than  $0.02^\circ$  over the entire energy range even in a field of 10 T.

### III. ELECTRONIC STRUCTURE

#### A. Theory

To discuss optical and magneto-optical data in terms of the electronic structure, the diagonal and off-diagonal elements of the complex conductivity tensor  $\underline{\sigma}$  have to be evaluated. For a cubic material with an applied magnetic field in the  $z$  direction,  $\underline{\sigma}$  has the following form:

$$\underline{\sigma} = \begin{pmatrix} \sigma_{xx} & \sigma_{xy} & 0 \\ -\sigma_{xy} & \sigma_{xx} & 0 \\ 0 & 0 & \sigma_{zz} \end{pmatrix}. \quad (1)$$

The tensor elements  $\sigma_{ij} = \sigma_{1ij} + i\sigma_{2ij}$  are complex functions which, in the approximation of momentum-independent matrix elements, can directly be related to the joint density of states. In first-order perturbation theory, the diagonal elements are independent and the off-diagonal elements are directly proportional to the sample magnetization.<sup>11</sup>

In a modified atomic model,<sup>12</sup> the total weights  $\langle \text{Re}\sigma_{xx} \rangle = \int \text{Re}\sigma_{xx} d\omega$  and  $\langle \text{Im}\sigma_{xy} \rangle = \int \text{Im}\sigma_{xy} d\omega$  for a given interband transition exhibit the following proportionalities:

$$\langle \text{Re}\sigma_{xx} \rangle \approx \omega_{\alpha\beta} |M|^2 J_{\alpha\beta}, \quad (2)$$

$$\langle \text{Im}\sigma_{xy} \rangle \approx \omega_{\alpha\beta} (|M_-|^2 - |M_+|^2) J_{\alpha\beta} \sigma_j. \quad (3)$$

Here,  $\omega_{\alpha\beta}$  is the transition energy,  $J_{\alpha\beta}$  is the integrated joint density of states,  $\sigma_j$  is the joint spin polarization and  $M$ ,  $M_+$ , and  $M_-$  are dipole matrix elements for unpolarized and right- and left-hand circularly polarized light, respectively.

For intraband transitions, the theory gives a proportionality of  $\sigma_{xy}$  to the free-electron concentration via the plasma frequency  $\omega_p^2 = 4\pi N e^2 / m^*$  and to the spin polarization  $\sigma_d$  of the conduction electrons. In addition,  $\sigma_{xy}$  is proportional to the strength of spin-orbit coupling  $P_0 / ev_0$ ,<sup>13</sup>

$$\sigma_{xy}(\omega) = \frac{\omega_p^2}{4\pi} \langle \sigma_d \rangle \left[ \frac{-\Omega}{\Omega^2 + (1/\tau + i\omega)^2} + \frac{|P_0|}{ev_0} \left[ 1 - \frac{i\omega(1/\tau + i\omega)}{\Omega^2 + (1/\tau + i\omega)^2} \right] \right]. \quad (4)$$

In this equation,  $\gamma = 1/\tau$  and  $\Omega$  are the relaxation and the skew-scattering frequency, respectively.

From the measured reflectivity  $R$  and its phase, obtained by Kramers-Kronig transformation,

$$\sigma_{xx}(\omega) = (\omega/4\pi) [2nk + i(n^2 - k^2 - 1)]$$

is computed.<sup>6</sup> The off-diagonal elements  $\sigma_{xy}$  are calculated from the Kerr rotation  $\theta_K$ , the Kerr ellipticity  $\epsilon_K$ , and the optical constants  $n$  and  $k$ ,<sup>14</sup>

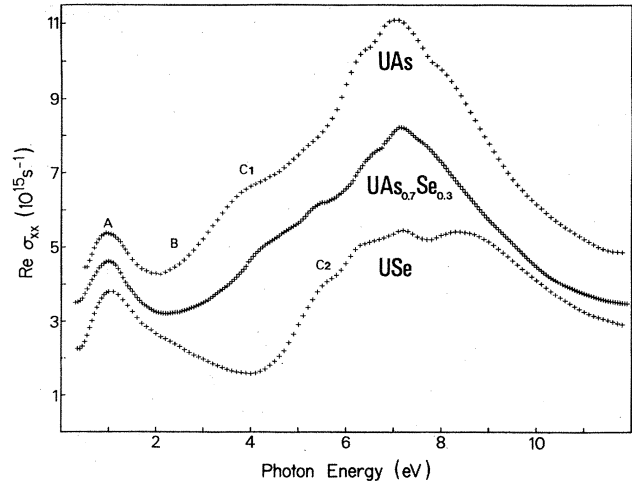


FIG. 1. Absorptive part of the diagonal conductivity of  $\text{UAs}$ ,  $\text{UAs}_{0.7}\text{Se}_{0.3}$ , and  $\text{USe}$  at room temperature and  $B=0$ . Consecutive curves are vertically shifted by one unit.

$$\sigma_{1xy} = \frac{\omega}{4\pi} [-\theta_K(3n^2k - k^3 - k) - \epsilon_K(n^3 - 3nk^2 - n)], \quad (5)$$

$$\sigma_{2xy} = \frac{\omega}{4\pi} [-\theta_K(n^3 - 3nk^2 - n) + \epsilon_K(3n^2k - k^3 - k)]. \quad (6)$$

#### B. Optical properties

The optical conductivity of  $\text{UAs}_{0.7}\text{Se}_{0.3}$  (Fig. 1) shows features which are typical for UX compounds ( $X=\text{S, Se, Te, P, As, and Sb}$ ).<sup>6</sup> The free-electron contribution is weak, relative to the expected number of conduction electrons, and is also highly damped. The plasma energy lies between the values observed for  $\text{UAs}$  and  $\text{USe}$ . Two strong interband transitions (peaks  $A$  and  $B$ ) dominate the low-energy conductivity, while the broad and structured absorption band around 7.5 eV is attributed to valence-band excitations.<sup>6</sup>

To compare with the magneto-optical data, we will focus on the low-energy range (0.5–6 eV). A quantitative analysis including a fit of the conductivity with Lorentz functions gives the following results (Fig. 1). (i) In all three compounds peak  $A$  has the same transition energy,  $\hbar\omega_A = (1.0 \pm 0.02)$  eV, the same width,  $\hbar\gamma \approx 1.15$  eV, and the same oscillator strength,  $f=0.9$ . This points to identical initial and final states for this excitation in the different compounds. (ii) Peak  $B$  decreases in oscillator strength by about a factor of 3 going from  $\text{USe}$  to  $\text{UAs}$ , while its energy,  $\hbar\omega_B \approx (2.4 \pm 0.2)$  eV, and its width,  $\hbar\gamma \approx (2 \pm 0.3)$  eV, remain constant. (iii) Substituting for As with Se, peak  $C1$  at about 4 eV in  $\text{UAs}$  seems to weaken at constant energy, and at about 5.5 eV a new peak,  $C2$ , develops.

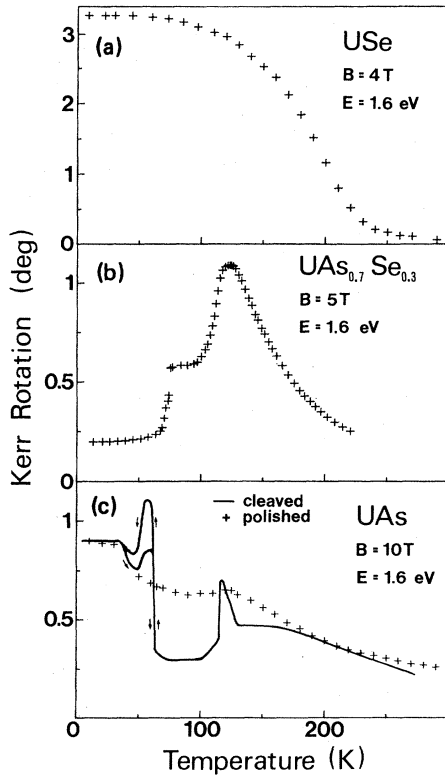


FIG. 2. Temperature dependence of  $\theta_K$  at  $\hbar\omega = 1.6\text{ eV}$  for (a) USe, (b)  $\text{UAs}_{0.7}\text{Se}_{0.3}$ , and (c) UAs. The applied field is the same as in the energy-dependent measurements of  $\theta_K$  and  $\epsilon_K$  displayed in Fig. 3.

### C. Magneto-optical properties

#### 1. Experimental results

Figure 2 enlightens the complex magnetic phase diagram in the system  $\text{UAs}_x\text{Se}_{1-x}$ . The simplest case is USe,

for which the temperature dependence of  $\theta_K$  shows a typical ferromagnetic behavior [Fig. 2(a)] with

$$M(100) = M(111)/\sqrt{3} = 1.06\mu_B/U$$

at 15 K and 4 T.<sup>5</sup> UAs orders antiferromagnetically and thus only very small magneto-optical effects are found in low fields. However, UAs undergoes a magnetic phase transition at 8.7 T (see also Sec. IV). In the high-field-induced ferrimagnetic phase, the magnetic moment reaches  $M(100) = 0.42\mu_B/U$  at 10 T and 20 K. Consequently, the observed Kerr rotation is about a factor of 3 smaller than in USe [Fig. 2(c)]. With increasing temperature different ferri- and antiferromagnetic phases can be observed; these will be discussed in detail in Sec. IV.

In a field of 5 T the mixed compound  $\text{UAs}_{0.7}\text{Se}_{0.3}$  shows four magnetic phases as a function of temperature [Fig. 2(b)]: paramagnetic behavior for  $T > T_N = 127\text{ K}$ , a ferromagnetic phase between  $T_N$  and about 115 K, and two different antiferromagnetic regions at lower temperatures.<sup>1</sup> The highest magnetic moment occurs in the ferromagnetic phase at 123 K and amounts to  $M(100) = 0.48\mu_B/U$ .

To obtain the highest resolution, the magneto-optical spectra to be reported have been measured at the temperature which gives the largest signal. Figure 3 displays these results for the three compounds. The spectra all look very similar, each with two structures in  $\theta_K$  and  $\epsilon_K$ . Yet, because  $\theta_K$  and  $\epsilon_K$  are linear combinations of absorptive and dispersive quantities, their interpretation in terms of the electronic structure is not straightforward. Instead, the real and imaginary part of the off-diagonal conductivity  $\sigma_{xy}$ , shown in Fig. 4, should be discussed.

Up to about 2.5 eV the off-diagonal conductivity of the three materials displays large similarities. For higher energies, no magneto-optical active excitations are observed in USe, but there appears a broad peak, C1, around 3.2 eV with increasing As concentration.

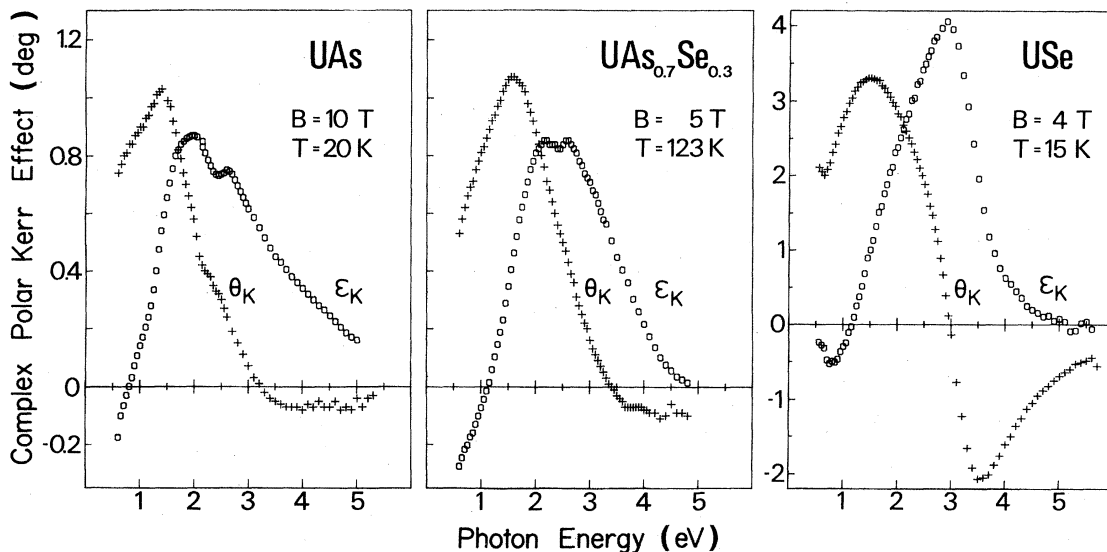


FIG. 3. Energy-dependent polar Kerr rotation  $\theta_K$  and Kerr ellipticity  $\epsilon_K$  for (100)-oriented cleaved single crystals of UAs,  $\text{UAs}_{0.7}\text{Se}_{0.3}$ , and USe. Note the change of the ordinate scale for USe.

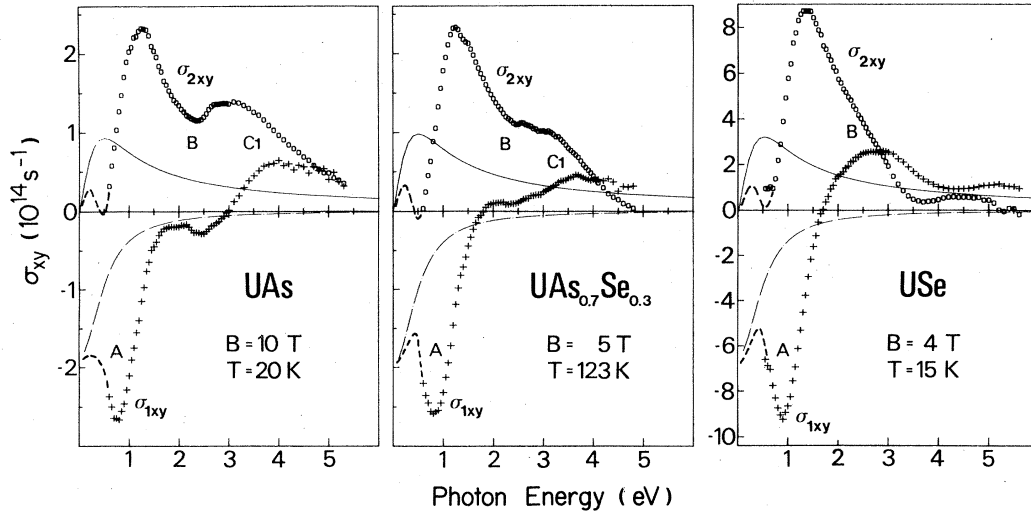


FIG. 4. Absorptive ( $\sigma_{2xy}$ ) and dispersive ( $\sigma_{1xy}$ ) part of the off-diagonal conductivity for (100)-oriented cleaved single crystals of UAs,  $\text{UAs}_{0.7}\text{Se}_{0.3}$ , and USe. The dashed line displays the extrapolation of  $\sigma_{xy}$  for  $\hbar\omega < 0.5$  eV obtained by Kramers-Kronig inversion (see text). The solid and dashed-dotted curves render visible the estimated free-electron contribution to  $\sigma_{1xy}$  and  $\sigma_{2xy}$ , respectively. Note the change of the ordinate scale for USe.

## 2. Analysis of the spectra

In Fig. 4 an extrapolation of  $\sigma_{xy}$  for energies less than 0.5 eV is included, taking advantage of the Kramers-Kronig relation between  $\sigma_{1xy}(\omega)$  and  $\sigma_{2xy}(\omega)$ . A comparison of the energy of peak *A* in  $\sigma_{xx}$  and  $\sigma_{xy}$  (Sec. III D) indicates that the line shape of this lowest-energy interband transition *A* has to be “diamagnetic,” i.e., it shows a bell-shaped form with a maximum in  $\sigma_{1xy}$  at  $\omega_A$  and  $\sigma_{2xy}(\omega_A) = 0$ . Consequently, the free-electron contribution to  $\sigma_{2xy}$  must be positive, which is equivalent to a negative spin polarization of the conduction electrons [Eq. (4)]. This holds for ferromagnetic USe and  $\text{UAs}_{0.7}\text{Se}_{0.3}$  as well as for ferrimagnetic UAs, and it constitutes the first experimental determination of the conduction-electron spin polarization for an uranium pnictide. It agrees with the result of a spin-polarized band-structure calculation for UP.<sup>15</sup> In the case of USe, the negative polarization is in qualitative agreement with a calculation for US (Ref. 8) and with spin-polarized photoemission results.<sup>16</sup>

To derive the size of the spin polarization from the free-electron contribution, several parameters occurring in Eq. (4) have to be estimated. First, comparing the two terms on the right-hand side of this equation, we note that at  $\hbar\omega = 1$  eV their ratio<sup>13</sup>  $(P_0/ev_0)/(\Omega/\omega^2)$  amounts to  $\approx 10$  in our compounds. Thus we neglect the first term in the following. Taking the same values as in US (Ref. 17) for the relaxation frequency  $\hbar\gamma$  and the spin-orbit contribution  $P_0/ev_0$ , the product of spin polarization and conduction-electron concentration is found to be  $-41$ ,  $-13$ , and  $-12$  % electrons/formula unit for USe,  $\text{UAs}_{0.7}\text{Se}_{0.3}$ , and UAs, respectively. The solid and dashed-dotted curves in Fig. 4 display the corresponding free-electron contributions to  $\sigma_{xy}$ . To obtain the size of the spin polarization alone, one needs to know the conduction-electron concentration. Assuming the same value for USe as for US (Ref. 17) and scaling, for

$\text{UAs}_{0.7}\text{Se}_{0.3}$  and UAs, the concentration with either the square of the plasma energy or with the intensity of the  $d \rightarrow f$  transition<sup>18</sup> within the  $\text{UAs}_x\text{Se}_{1-x}$  series, the values  $-35\%$ ,  $-20\%$ , and  $-30\%$  are derived for the three compounds with increasing  $x$  and the magnetic fields given in Fig. 4.

The pure interband contribution to  $\sigma_{xy}(\omega)$  is the difference of the measured  $\sigma_{xy}(\omega)$  and the free-electron contribution. It is dominated by a diamagnetic transition *A* with exactly the same line width [full width at half maximum (FWHM)  $\approx 0.7$  eV] but different transition energies for USe,  $\text{UAs}_{0.7}\text{Se}_{0.3}$ , and UAs (Table I). The total weight is about a factor of 4 less for UAs than for USe, which corresponds approximately to the ratio of the total magnetic moments.

Moving to higher photon energies, we find at  $\approx 2.3$  eV a peak *B* with a “paramagnetic” line shape in all materials. The total weight of this peak decreases from USe to UAs by a factor of about 6. Peak *C1* in Fig. 4 has also a “paramagnetic” line shape, but is only present in the As-rich samples of  $\text{UAs}_x\text{Se}_{1-x}$ . The width of this transition increases with the As concentration. Its energy agrees roughly with the energy of peak *C1* in the diagonal conductivity (Fig. 1). Peak *C2*, however, which is clearly resolved in  $\sigma_{1xx}$  for USe around 5 eV, has no corresponding signal in  $\sigma_{xy}$ .

TABLE I. Observed transition energy  $\hbar\omega_A$  in  $\sigma_{xy}$  and integrated weight  $\langle \text{Im}\sigma_{2xy} \rangle$  of transition *A* in the magnetically ordered phases of UAs,  $\text{UAs}_{0.7}\text{Se}_{0.3}$ , and USe. The experimental conditions are given in Figs. 3 and 4.

	UAs	$\text{UAs}_{0.7}\text{Se}_{0.3}$	USe
$\hbar\omega_A$ (eV)	0.82	0.86	0.94
$\langle \text{Im}\sigma_{xy} \rangle$ ( $10^{29} \text{ sec}^{-2}$ )	2.3	2.3	9.0

### D. Discussion

The electronic configurations of U ( $5f^36d^17s^2$ ), As ( $4p^3$ ), and Se ( $4p^4$ ) suggest that the density of states around  $E_F$  will be dominated by a nearly-filled  $p$  valence band, a  $d$  conduction band, and narrow  $f$  states. This general picture is supported by different band-structure calculations.<sup>9,15,19</sup> In addition, a cluster calculation has shown that due to a strong  $f$ - $d$  hybridization, a pronounced peak in the occupied  $d$  density can be expected.<sup>8</sup> The degree of  $f$ -localization, however, is still the subject of a keen debate.

In  $\sigma_{xx}$  as well as in  $\sigma_{xy}$ , we assign peak  $A$  to a transition from a narrow  $f$  band at  $E_F$  into  $d$  states. This interpretation is substantiated by the following arguments. (i) Peak  $A$  is present in the optical spectrum ( $\sigma_{xx}$ ) of UAs as well as that of USe with the same line shape and the same oscillator strength. (ii) In  $\sigma_{xy}$  this transition again has the same line shape, and the size of the peak is proportional to the magnetic moments in the different compounds. (iii) The large size of the magneto-optical response points to the excitation of "magnetic" electrons with large spin polarization. (iv) Equations (2) and (3) describe the experimental oscillator strengths and line shapes for  $\sigma_{1xx}$  and  $\sigma_{2xy}$ .<sup>20</sup> This modified atomic-model calculation<sup>12,17</sup> results in an  $f$  occupancy  $n_f$  which is less than the expected occupancy by about a factor of 2, assuming  $n_f = 4 - n_d$  in USe and  $n_f = 3 - n_d$  in UAs. This is a clear indication of the presence of non-negligible correlation effects<sup>21</sup> in the narrow  $f$  band. (v) The absence of any fine structure in  $\sigma_{xy}$ , which would be expected for strictly localized  $f$  states,<sup>22,23</sup> points, on the other hand, to an  $f$ -band width in excess of typical spin-orbit energies.

One further interesting feature of the  $f \rightarrow d$  transition in  $\text{UAs}_x\text{Se}_{1-x}$  is the different resonance energy  $\hbar\omega_A$  in  $\sigma_{xx}$ , observed at  $T=300$  K for  $B=0$ , and in  $\sigma_{xy}$ , observed for  $T < T_{C,N}$  and  $B \neq 0$ . Such large magnetization-induced red shifts were up to now only observed in some ferromagnetic and antiferromagnetic semiconductors.<sup>24</sup> The maximum shift is 0.3 eV in EuO. Yet, it was found for EuO doped with Gd that the red shift decreases with increasing conduction-electron concentration.<sup>25</sup> Applying a similar argument to our  $\text{UAs}_x\text{Se}_{1-x}$  system, UAs should exhibit the largest red shift, which is actually the case. Unfortunately, the evolution of the total 0.17-eV shift in UAs as a function of magnetization is hard to follow up in detail because of the complex magnetic phase diagram of UAs and the rather small magneto-optical signals in the antiferromagnetic phases. This problem is less difficult in  $\text{UAs}_x\text{Se}_{1-x}$  and we have measured the Kerr-rotation maximum, which corresponds to peak  $A$  in  $\sigma_{xy}$ , as a function of magnetization. Figure 5 displays the photon-energy dependence of the Kerr rotation at  $T=123$  K  $\approx T_N$  normalized to its maximum value for different magnetic fields. We observe that the red shift of the  $f \rightarrow d$  transition saturates at a field of  $\approx 5$  T and amounts to about 0.14 eV. To our knowledge, the As-rich  $\text{UAs}_x\text{Se}_{1-x}$  compounds are the first metals to show such a striking magneto-optical effect.

The observed red shift together with the observed negative conduction-electron spin polarization leads to new conclusions about the  $f$  moment. The model of an

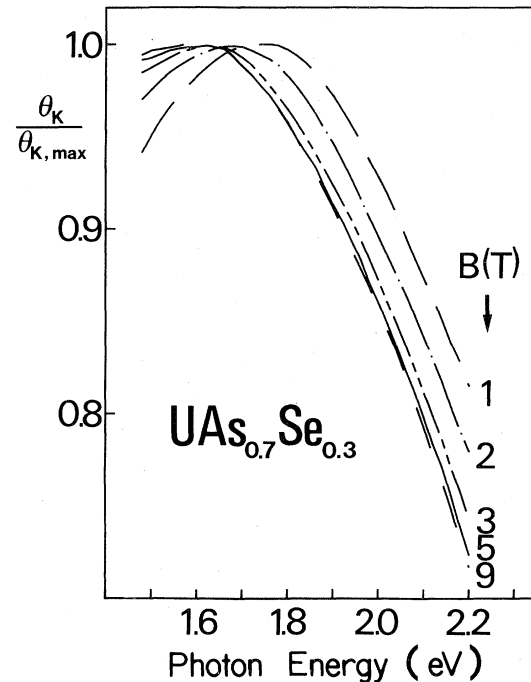


FIG. 5. Normalized Kerr rotation of  $\text{UAs}_{0.7}\text{Se}_{0.3}$  at  $T=123$  K for different applied fields in the energy range of maximum rotation (transition  $A$ ).

exchange-induced  $d$ -band splitting to explain the red shift requires parallel  $d$  and  $f$  spins.<sup>24</sup> On the other hand, the negative spin polarization necessitates that the  $d$  spin is antiparallel to the total  $f$  moment. Both results are only compatible if the total  $f$  moment consists of antiparallel orbital and spin components with a dominating orbital part. This is a direct experimental corroboration of a recent theoretical work on UN proposing a dominant orbital-moment contribution to the  $5f$ -band magnetism.<sup>26</sup>

The initial and/or final states of transition  $B$  in  $\sigma_{xx}$  and  $\sigma_{xy}$  have to possess a net spin polarization which is responsible for the observed large magneto-optical response. In addition the oscillator strength decreases nearly proportional to  $\omega_p^2$ , i.e., it is proportional to the number of  $d$  electrons. Both facts point to an interpretation in terms of a  $d \rightarrow f$  transition. The occurrence of a strong  $d \rightarrow f$  transition, however, can only be expected if the  $f$  states are not localized.<sup>21</sup> Thus the observation of this transition with equivalent strength in  $\text{UAs}_x\text{Se}_{1-x}$  corroborates similar  $f$  delocalization for different  $x$ . On the other hand, the same excitation shows a drastic decrease in oscillator strength along the uranium chalcogenide and pnictide series, indicating the increase of the  $f$  localization for UX compounds with heavier cations.<sup>27</sup>

At first sight the strong magneto-optical response of peak  $C1$  around 3.3 eV in  $\sigma_{xy}$  (Fig. 4) of UAs and its absence for USe is an unexpected result. To understand this behavior, let us examine somewhat closer the  $p$  valence band in the system under discussion.

Using band-structure calculations<sup>8,9,19</sup> we find the valence band of UAs and USe centered at binding energies of about 3 and 5 eV, respectively. In addition, due to a strong admixture of some  $f$  and merely  $d$  states to the  $p$

states, a nonuniform distribution of angular momentum throughout the band is predicted for the pnictides with more high- $l$  states at the top and more low- $l$  states at the bottom.<sup>9</sup> This admixture is smaller for the chalcogenides because of the higher  $p$  binding energies and the smaller charge transfer necessary to fill the valence band.

Thus peaks C1 and C2 in  $\sigma_{xx}$  (Fig. 1) are interpreted as the onset of excitations from the top of the valence band. These transitions are magneto-optically active only for strong  $f, d$  admixtures, and we assign peak C1 in  $\sigma_{xy}$  (Fig. 4) to a  $pd \rightarrow f$  transition.

Comparing our results with different photoemission studies on UAs and USe, we find, in general, good agreement.<sup>7,16,28</sup> In particular, the energy separation of high- $l$  and low- $l$  valence states for the uranium pnictides has also been deduced from energy-dependent ultraviolet-photoemission-spectroscopy (UPS) measurements.<sup>28</sup> On the other hand, in a recent UPS study on  $\text{UAs}_x\text{Se}_{1-x}$ ,<sup>29</sup> two emission peaks, one close to  $E_F$  and one 0.7 eV below  $E_F$ , have been interpreted as a final-state splitting of localized  $5f$  states, and large differences in the  $f$  density of states between the chalcogenide and the pnictide have been claimed to exist. However, an examination of the experimental UPS results merely shows an increase of the peak intensity at 0.7 eV binding energy going from UAs to USe, which in light of our magneto-optical measurements reflects an increase of the occupancy of the  $6d$  conduction band.<sup>8</sup>

#### IV. MAGNETIC STRUCTURE OF UAs

Among the UX compounds, UAs is certainly the compound which exhibits the most complex magnetic behavior.<sup>3</sup> To demonstrate magneto-optics as a powerful tool for the investigation of magnetic phase transitions, we have reexamined the magnetic phase diagram of UAs in applied fields up to 10 T. In Fig. 6 the computer graph of the measured temperature dependence of the Kerr rotation is reproduced for a (001) cleaved single crystal with the applied magnetic field along [100] as a parameter. Around  $T_N = 124.5$  K one observes, at medium fields, the appearance of an intermediate phase with higher magnetization than the surrounding paramagnetic and antifer-

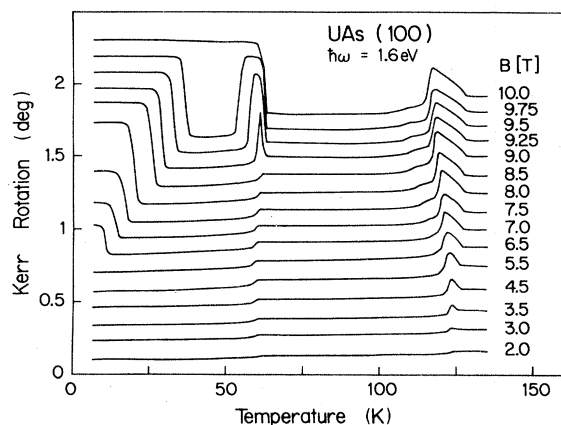


FIG. 6. Temperature dependence of  $\theta_K$  measured on a cleaved UAs single crystal in fields up to 10 T and decreasing temperature. Consecutive curves are shifted by  $0.1^\circ$  for clarity.

romagnetic (type-I) phases. This intermediate phase has been identified by neutron scattering to be single- $\vec{k}$  ferrimagnetic with a  $++-$  stacking of (001) ferromagnetic planes.<sup>3</sup> The triple point of coexisting paramagnetic, antiferromagnetic, and ferrimagnetic phases is found at  $B=3$  T and  $T=124.5$  K. For  $B < 9$  T at  $T \simeq 62$  K Fig. 6 exhibits the phase transition to the double- $\vec{k}$  antiferromagnetic type-IA structure. This transition is accompanied by a 10% decrease in magnetization which is due to the jump of the magnetic moments from a (001) to a (110) direction.<sup>3</sup> At  $B=9.2$  T and  $T=61.5$  K we find the triple point of two antiferromagnetic phases (types I and IA) and another ferrimagnetic phase with a double- $\vec{k}$  structure.

In addition to the described transitions, which have been observed on several cleaved UAs single crystals, one sample showed at 10 T between 53 and 62 K one further magnetic structure displaying a strong hysteresis [as can be recognized in Fig. 2(c)]. The magnetic moment at 10 T in this additional phase, which was also not found by neutron scattering in all investigated samples,<sup>3</sup> is estimated from our magneto-optical data to be  $0.53\mu_B/\text{U}$ . This value corresponds to the magnetization expected theoretically for the  $2\vec{k}$  ferrimagnetic structure.<sup>3</sup> The reduced experimental value of  $0.42\mu_B/\text{U}$  found for  $T < 53$  K is explained<sup>3</sup> by defects in the stacking sequence of ferromagnetic sheets. The introduction of stacking defects is accompanied by a change in magnetization, but the wave vector remains unchanged with the neutron experiments. The observation of the same size of the Kerr rotation for both kinds of UAs crystals at 10 T and  $T < 40$  K indicates that only the crystals with the additional phase between 54 and 62 K at 10 T possess a  $2\vec{k}$  ferrimagnetic structure without stacking faults. Our observation of dramatic changes of the magnetic phase diagram upon polishing also suggests that the different magnetic behavior of the two kinds of UAs single crystals reflects the large sensitivity of the magnetic properties of this material to internal strain and stress.

In Fig. 2 we have added the field-cooled temperature dependence of  $\theta_K$  at 10 T measured on a polished surface. We observe that  $T_N$  as well as the size of the rotation in the ferrimagnetic phases remain unchanged compared with the cleaved sample, but  $\theta_K$  (or the magnetization) increases quite strongly in the antiferromagnetic and paramagnetic regions. These changes of the magnetic phase diagram have to be related to the deformation of the regular lattice by the polishing process. Phase transitions from semiconducting to metallic SmS, which necessitate about 6 kbar of hydrostatic pressure, are known to occur also upon polishing.<sup>30</sup> On the other hand, magnetization measurements at hydrostatic pressure in fields up to 7 T on UAs have shown that only minor variations of the transition temperatures occur up to 8 kbar.<sup>31</sup> The magnetization of the antiferromagnetic phases was shown to be independent of pressure. Thus in the case of UAs the effect of polishing cannot simply be correlated with the application of hydrostatic pressure, but more complicated phenomena such as alterations of exchange energies have to be evoked.

## V. CONCLUSIONS

We have shown that the  $f$  states give rise to the same line shape and similar intensities for the chalcogenide and the pnictide, and that no major differences exist compared to US.<sup>17</sup>

The diagonal and off-diagonal conductivity tensor elements have been interpreted in a uniform manner with the assumption of narrow occupied  $d$ - and  $f$ -band states. The strong hybridization of the valence  $p$  band with electronic states of high orbital momentum for the uranium pnictides manifests itself in a further transition with very strong magneto-optical response.

It is shown that the strong exchange between  $f$  spins and conduction electrons results in a magnetic red shift of

the  $f \rightarrow d$  transition. In light of the observed increase of the shift with a decreasing number of free carriers, we expect to find still larger values for, e.g., USb. The red shift and the negative spin polarization of the  $d$  electrons indicates antiparallel orbital and spin contributions to the total  $f$  moment with a dominating orbital part.

## ACKNOWLEDGMENTS

The authors are indebted to Professor Dr. P. Wachter for his interest and support of this work. The technical assistance of P. Dekumbis, K. Mattenberger, and J. Müller is gratefully acknowledged. This work was financially supported by the Swiss National Science Foundation.

- <sup>1</sup>O. Vogt and H. Bartholin, *J. Magn. Magn. Mater.* **29**, 291 (1982).
- <sup>2</sup>G. H. Lander, M. H. Müller, and J. F. Reddy, *Phys. Rev. B* **6**, 1880 (1972).
- <sup>3</sup>J. Rossat-Mignod, P. Burllet, S. Quézel, O. Vogt, and H. Bartholin, in *Crystalline Electric Field Effects in  $f$ -Electron Magnetism*, edited by R. P. Guertin, W. Suski, Z. Sołnierk (Plenum, New York, 1982).
- <sup>4</sup>G. Busch, O. Vogt, and H. Bartholin, *J. Phys. (Paris) Colloq.* **40**, C4-64 (1979).
- <sup>5</sup>G. Busch and O. Vogt, *J. Less-Common Metals* **62**, 335 (1978).
- <sup>6</sup>J. Schoenes, *Phys. Rep.* **66**, 187 (1980).
- <sup>7</sup>Y. Baer, *Physica* **102B**, 104 (1980).
- <sup>8</sup>J. Schoenes, O. Vogt, and J. Keller, *Solid State Commun.* **32**, 873 (1979).
- <sup>9</sup>M. S. S. Brooks and D. Glötzel, *Physica* **102B**, 51 (1980).
- <sup>10</sup>The reflectivities of UAs and USe have already been published in Ref. 6.
- <sup>11</sup>W. A. Crossley, R. W. Cooper, J. L. Page, and R. P. van Staple, *Phys. Rev.* **181**, 896 (1969).
- <sup>12</sup>J. L. Erskine and E. A. Stern, *Phys. Rev. B* **8**, 1239 (1973). Because of a different definition of the optical constants [ $\epsilon_1 - i\epsilon_2 = (n - ik)^2$ ], our formula (4) has the opposite sign.
- <sup>13</sup>W. Reim, O. E. Hüsler, J. Schoenes, E. Kaldis, P. Wachter, and K. Seiler, *J. Appl. Phys.* (in press).
- <sup>14</sup>X. X. Zhang, J. Schoenes, W. Reim, and P. Wachter, *J. Phys. C* **16**, 6055 (1983).
- <sup>15</sup>M. S. S. Brooks (private communication).
- <sup>16</sup>F. Greuter, W. Eib, M. Erbudak, F. Meier, and B. Reihl, *J. Appl. Phys.* **50**, 7483 (1979).
- <sup>17</sup>W. Reim, J. Schoenes, and O. Vogt, *Solid State Commun.* **47**, 597 (1983).
- <sup>18</sup>Peak  $B$  is shown to be a  $d \rightarrow f$  excitation in Sec. III C.
- <sup>19</sup>P. Weinberger and R. Podlucky, *Phys. Rev. B* **22**, 645 (1980).
- <sup>20</sup>The parameters in this calculation are the overlap integral of the  $f$  and  $d$  wave function  $R_{df}$ , and the spin-orbit parameter. The first has been calculated by Brooks for USe as well as for UAs in a linear muffin-tin orbital band-structure calculation, giving for both materials a value  $R_{df} = 6.8 \times 10^{17} \text{ cm}^2$ . The spin-orbit parameter was taken from F. Herman and S. Skillman, *Atomic Structure Calculations* (Prentice-Hall, Englewood Cliffs, N.J., 1963).
- <sup>21</sup>For strictly localized  $f$  electrons (i.e.,  $\text{UO}_2$ ), the calculation results in an  $f$  occupancy which is too small by a factor of 10. See J. Schoenes, *J. Phys. (Paris) Colloq.* **5**, C-31 (1980); in *Proceedings of the NATO Summer Institute on Moment Formation in Solids*, edited by W.J.L. Buyers (Plenum, New York, 1984).
- <sup>22</sup>W. Reim and J. Schoenes, *Solid State Commun.* **39**, 1101 (1981).
- <sup>23</sup>J. Schoenes, *Z. Phys. B* **20**, 345 (1975).
- <sup>24</sup>P. Wachter, in *Handbook of Physics and Chemistry of Rare Earths*, edited by K. A. Gschneider, Jr. and L. Eyring (North Holland, Amsterdam, 1979).
- <sup>25</sup>J. Schoenes and P. Wachter, *Phys. Rev. B* **9**, 3097 (1974).
- <sup>26</sup>M. S. S. Brooks and P. J. Kelly, *Phys. Rev. Lett.* **51**, 1708 (1983).
- <sup>27</sup>W. Reim, J. Schoenes, and O. Vogt, *J. Appl. Phys.* (in press).
- <sup>28</sup>F. Greuter, E. Hauser, P. Oelhafen, H. J. Güntherodt, B. Reihl, and O. Vogt, *Physica* **102B**, 117 (1980).
- <sup>29</sup>B. Reihl, N. Martensson, and O. Vogt, *J. Appl. Phys.* **53**, 2008 (1982).
- <sup>30</sup>V. P. Zhuze, A. V. Golubkov, E. V. Goucharova, T. I. Komarova, and V. M. Sergeeva, *Fiz. Tverd. Tela (Leningrad)* **6**, 268 (1964) [*Sov. Phys.—Solid State* **6**, 213 (1964)].
- <sup>31</sup>J. Rossat-Mignod, P. Burllet, H. Bartholin, R. Tchapoutian, O. Vogt, C. Vettier, and R. Lagnier, *Physica* **102B**, 177 (1980).